Vibronic spectra of aluminium monochloride relevant to circumstellar molecule*

Jian-Gang Xu(徐建刚), Cong-Ying Zhang(张聪颖), and Yun-Guang Zhang(张云光)†

School of Science, Xi'an University of Posts and Telecommunications, Xi'an 710121, *China*

(Received 8 November 2019; revised manuscript received 13 January 2020; accepted manuscript online 16 January 2020)

The $A^1\Pi \rightarrow X^1\Sigma^+$ transition system of aluminium monochloride is determined by using *ab initio* quantum chemistry. Based on the multi-reference configuration interaction method in conjugate to the Davidson correction (MRCI + Q), the potential energy curves (PECs) of the three electronic states are obtained. Transition dipole moments (TDMs) and the vibrational energy levels are studied by employing the aug-cc-pwCV5Z-DK basis set with 4220-active space. The rovibrational constants are first determined from the analytic potential by solving the rovibrational Schrödinger equation, and then the spectroscopic constants are determined by fitting the vibrational levels, and these values are well consistent with the experimental data. The effect of spin–orbit coupling (SOC) on the spectra and vibrational properties are evaluated. The results show that the SOC effect has almost no influence on the spectroscopic constants of AlCl molecules. For the $A^1\Pi \rightarrow X^1\Sigma^+$ transition, the highly diagonalized Frank–Condon factor (FCF) is f_{00}=0.9988. Additionally, Einstein coefficients and radiative lifetimes are studied, where the vibrational bands include $v'' = 0$–$19 \rightarrow v' = 0$–9. The ro-vibrational intensity is calculated at a temperature of 296 K, which can have certain astrophysical applications. At present, there is no report on the calculation of AlCl ro-vibrational intensity, so we hope that our results will be useful in analyzing the interstellar AlCl based on the absorption from $A^1\Pi \rightarrow X^1\Sigma^+$.

Keywords: spectroscopic constants, radiative lifetime, Franck–Condon factor, transition intensity

PACS: 31.15.A–, 37.10.Mn, 87.80.Cc **DOI:** 10.1088/1674-1056/ab6c46

1. Introduction

Aluminium monochloride (AlCl) molecule is very important in astrophysics. So far, several research groups have explored it in deep space. In 1973, Tsuji[1] first predicted the existence of AlCl in the atmosphere of the carbon-rich and oxygen-rich stellar by themal equilibrium calculations. In 1987, the molecule at outer circumstellar envelope of carbon-rich star IRC + 10216 was successfully detected through microwave spectroscopy by Cernicharo and Guelin.[2] Ziurys[3] also positively confirmed it in 2006. In 2012, Agúndez *et al.*[4] not only found a large amount of IRC + 10216 in the cold outer shell, but also studied the abundance of IRC + 10216 in inner circumstellar molecular layers, and reported that the abundance of AlCl relative to H_2 was 7×10^{-8}. In O-rich stars, AlCl has also been observed by using ALMA submillimeter telescope array by Decin *et al.*[5] in 2017, who reported their findings in the circumstellar envelope of the red asymptotic giant branch stars IK Tau and R Dor. In addition, AlCl may also be detected in the photosphere of the Sun. The solar abundance of Al and Cl element have been estimated by Asplund *et al.*,[6] which makes it possible to detect AlCl in the Sun. In the various studies of the astronomy, the accurate spectroscopic constants, transition probabilities of emissions, and vibronic spectra of this molecule are necessary. Therefore a lot of experiments and theoretical researches have been carried out on this molecule.

Bhaduri and Fowler,[7] and Mahanti[8] first studied AlCl in experiment. After these pioneering observations, several experimental studies were carried out on AlCl. The rotational transitions of the millimeter region were gauged by Wyse and Gordy,[9] and a high-resolution emission spectrum at 20 μm was reported by Hedderich *et al.*[10] The dissociation energy $D_0 = 5.25 \pm 0.01$ eV was assessed from the thermochemical measurements by Hildenbrand and Theard[11] and optical experimental data by Ram *et al.*,[12] which shows that the ground state has a well depth. In addition, there were some experimental researches of the AlCl excited states from singlet–singlet and triplet–singlet systems. Ram *et al.*[12] have measured a rotational structure of 18 bands for the $A^1\Pi \rightarrow X^1\Sigma^+$ system containing $0 \le v' \le 10$ and $0 \le v'' \le 15$. The $A^1\Pi \rightarrow X^1\Sigma^+$ system was reported between 2500 Å and 2850 Å by Mahieu *et al.*,[13] which includes 29 bands with $2 \le v' \le 10$ and $0 \le v'' \le 16$. The 0–0 band of the $a^3\Pi \rightarrow X^1\Sigma^+$ transition has also been obtained at high resolution, and its rotational structure has been explicitly analyzed.[12–15]

Some theoretical calculations have also been carried out for AlCl molecule. Langhoff *et al.*[16] obtained the potential energy curves (PECs) of $A^1\Pi$ and $X^1\Sigma^+$ states and the moment functions of $A^1\Pi \rightarrow X^1\Sigma^+$ transition. Brites *et al.*[17] calculated the spectroscopic constants of $X^1\Sigma^+$, $A^1\Pi$, and $a^3\Pi$ states by using the multireference configuration interaction (MRCI) approach. Moreover, the values of transition energy

*Project supported by the National Natural Science Foundation of China (Grant No. 61705182).

†Corresponding author. E-mail: zygsr2010@163.com

© 2020 Chinese Physical Society and IOP Publishing Ltd

and radiative lifetime for $A^1\Pi \rightarrow X^1\Sigma^+$ system were also acquired by using *ab initio* method.[16,17] Recently, Yousefi and Bernath[18] have combined the AWCV5Z basis set with active space (6330) to compute spectroscopic constants and vibrational levels of the ground state. In addition, the PECs and transition dipole moments (TDMs) for $X^1\Sigma^+$, $A^1\Pi$, and $a^3\Pi$ states were studied with ACVQZ basis set, and the spin–orbit coupling (SOC) effects were considered at the MRCI level.[19] The Franck–Condon factors (FCFs) and emission rates were generated from $v = 0$, 1 levels of high state and $v = 0$–3 levels of the low state for $A^1\Pi_1 \rightarrow X^1\Sigma^+_{0^+}$, $A^1\Pi_1 \rightarrow a^3\Pi_{0^+,1}$, and $a^3\Pi_{0^+,1} \rightarrow X^1\Sigma^+_{0^+}$ transitions.

As mentioned above, some emission bands of $A^1\Pi \rightarrow X^1\Sigma^+$ transition were gauged. So far, although many spectroscopic constants have been calculated and some bands of this molecule have been studied. However, the systematic and accurate study of AlCl molecule is scarce. The research of SOC effect and transition properties is very important for molecular spectroscopy. It is necessary to consider this effect in the calculation. For these reasons, the transition probabilities and radiative lifetimes between $A^1\Pi$ and $X^1\Sigma^+$ states are studied in detail by using highly accurate MRCI approach with aug-cc-pwCV5Z-DK (AWCV5Z-DK) basis set. And finally, line intensity is obtained based on these results. In this paper, we depict the computational theory and approach in Section 2. In Section 3, the results and discussion are reported and lines intensity of the $A^1\Pi \rightarrow X^1\Sigma^+$ transition is outlined. Finally, the conclusion is presented in Section 4.

2. Theory and method

The *ab initio* calculations are implemented with the MOLPRO 2018 program package.[20] First of all, the spin-restricted Hartree–Fock method is used to calculate the $X^1\Sigma^+$ state energy. Based on these results, the initial values for orbital optimization of complete active space self-consistent-field (CASSCF) are obtained. Then, the multi-reference wave function[21,22] is carried out by the CASSCF method. Finally, the high-level MRCI together includes the Davidson correction (MRCI + Q), and the CASSCF wave functions are used to calculate the energy as a zero-order function.[23–25] The scalar relativistic corrections are performed by the third-order Douglas–Kroll Hamilton.[26,27] On the MRCI + Q level,[28] the SOC effect is assessed by Breit–Pauli operators. The above method has been well applied to several kinds of interstellar molecules.[29–32]

All calculations are performed in the C_{2v} point group, which has four irreducible representations (A_1, B_1, B_2, and A_2). The A_1 irreducible representation yields Σ^+ state and a component of Δ state, the B_1 and B_2 provide the Π state, and the A_2 yields the Σ^- state and the other component of Δ state. In the CASSCF calculation, eight molecular orbitals are put into active space ($7\sigma 8\sigma 3\pi_x 3\pi_y 9\sigma 4\pi_x 4\pi_y 10\sigma$), including four A_1, two B_1, and two B_2 molecular symmetry orbitals, which correspond to the 3s3p shells of the Al and Cl atom. In other words, ten electrons are distributed in one (4, 2, 2, 0) active space. In the following MRCI + Q step, the $1s^2 2s^2 2p^6$ shell of Al and Cl are used for core-valence correlation, *i.e.*, there are a total of 30 electrons in the calculations of correlation energy. The AWCV5Z-DK basis set is chosen for Al and Cl[32–35] because the core–valence correlation is essential for the accurate calculations.

The adiabatic PEC of the electronic state for AlCl molecule is composed of 146 single points in energy, with internuclear distances ranging from 1 Å to 8 Å. In order to obtain precise results, the interval value close to the equilibrium bond distance is reduced to 0.02 Å. Transition dipole moments (TDMs) and permanent dipole moments (PDMs) are also calculated in the same way. On this basis, spectroscopic constants are confirmed by solving the radial Schrödinger equation with the LEVEL program.[36]

The Einstein spontaneous emission coefficient $A_{v'v''}$ from upper electronic state level (v', J') to lower state level (v'', J'') is estimated by[37]

$$A_{v'v''} = 3.1361891 \times 10^{-7} \frac{S(J', J'')}{2J'+1} \nu^3 \left\langle \Psi_{v',J'} \middle| M(r) \middle| \Psi_{v'',J''} \right\rangle, \quad (1)$$

where $M(r)$ denotes the dipole moment in units of D, $S(J', J'')$ is the Hönl–London rotational intensity factor, ν is the wavenumber of transition in units of cm^{-1}, $\Psi_{v',J'}$ and $\Psi_{v'',J''}$ are normalized radical wave function for upper and lower states, respectively. The radiative lifetime can be computed by the reciprocal of the Einstein coefficient of total spontaneous emission as follows:

$$\tau = 1/\sum A_{v'v''}. \quad (2)$$

The conventional FCF is the square of the matrix element of the zeroth power of radial variable and expressed as[36]

$$q_{v'v''} = \left| \left\langle \Psi_{v',J'} / \Psi_{v'',J''} \right\rangle \right|^2. \quad (3)$$

The transition intensity of vibrational band spectrum is proportional to FCF as follows:[38]

$$I_{v'v''} \propto q_{v'v''}. \quad (4)$$

And that is, the relative transition intensity can also be calculated by the FCF for spontaneous emission.

3. Results and discussion

3.1. The PECs and spectroscopic constants of Λ–S states

In this paper, the PECs of three lowest Λ–S states ($X^1\Sigma^+$, $a^3\Pi$, and $A^1\Pi$) are studied and the results are shown in Fig. 1. It can be seen that the three states are typical bound states, and the dissociation asymptote is $Al(^2P_u) + Cl(^2P_u)$. Through

the LEVEL8.2 program, the spectroscopic constants containing the electronic transition energy (T_e), harmonic frequency (ω_e), equilibrium bond distance (R_e), anharmonic vibrational frequency ($\omega_e\chi_e$), rotational constants (B_e), and dissociation energy (D_e) are calculated for AlCl as shown in Table 1. For comparison, some other relevant calculated and experimental data of these three states are also listed in the table.

So far, the spectroscopic constants of AlCl have been studied extensively both theoretically[12,16–19,39] and experimentally.[9,10,13,40] For the ground state, Yousefi and Bernath[18] calculated the equilibrium bond distance R_e to be 2.1283 Å by using AWCV5Z basis set with 6330-active space, which is better consistent with the experimental value,[9,10,13,40] Obviously, the larger active space can gain more accurate results on the same basis set. Moreover, it shows that the AWCV5Z basis set can better reflect the core–valence correlation. Our harmonic frequency ω_e is 481.83 cm^{-1}, the absolute errors are only 0.16 cm^{-1}, 0.53 cm^{-1}, 0.43 cm^{-1}, and 0.0553 cm^{-1} obtained by separately comparing the experimental results,[9,10,13,40] indicating that our result is closer to the experimental value than others. The value of $\omega_e\chi_e = 2.0112$ cm^{-1} is also in good accordance with experimental data,[9,10,13,40] which has an effect on the vibrational levels. That is, the more reliable vibrational levels are obtained from the precise value of $\omega_e\chi_e$.

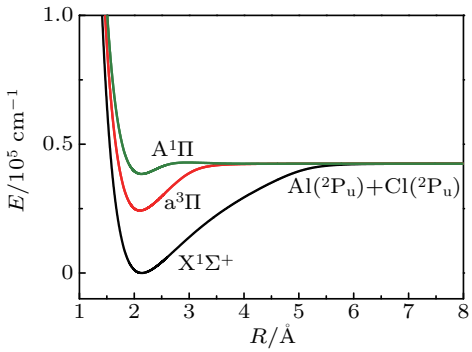

Fig. 1. Potential energy curves of $X^1\Sigma^+$, $a^3\Pi$, and $A^1\Pi$ states.

Table 1. Spectroscopic constants of $X^1\Sigma^+$, $a^3\Pi$, and $A^1\Pi$ states.

States	T_e/cm^{-1}	R_e/Å	ω_e/cm^{-1}	$\omega_e\chi_e$/cm^{-1}	B_e/cm^{-1}	D_e/eV	References
$X^1\Sigma^+$	0	2.1366	481.83	2.0112	0.2425	5.2619	this work
	240.162	–	–	–	0.2439	–	Cal[12]
	–	2.140	500	–	–	5.27	Cal[16]
	–	2.140	484.5	6.47	0.2418	–	Cal[17]
	0	2.145	478.36	1.95	0.2406	5.22	Cal[39]
	0	2.1374	478.13	–	0.2408	5.2142	Cal[19]
	–	2.1283	484.8065	2.06968	0.2441	–	Cal[18]
	–	2.1301	481.67	2.07	0.2439	–	Exp[9]
	0	2.1301	481.30	1.95	0.2439	5.1498	Exp[40]
	–	–	481.4	2.037	–	–	Exp[13]
	–	2.1301	481.7747	2.1018	0.2439	5.1201	Exp[10]
$a^3\Pi$	24223.5201	2.1035	527.37	2.6540	0.2501	2.2606	this work
	24793.105	–	–	–	0.2524	–	Cal[12]
	–	2.107	519.1	0.52	0.2494	–	Cal[17]
	24057	2.112	523.36	2.61	0.2481	2.24	Cal[39]
	23959.87	2.1050	525.68	–	0.2483	2.2462	Cal[19]
	–	2.10	524.35	2.175	0.250	–	Exp[40]
$A^1\Pi$	38436.3652	2.1324	453.43	8.4793	0.2435	0.4960	this work
	38237.0005	–	–	–	0.2454	–	Cal[12]
	38656	2.138	476	–	–	–	Cal[16]
	–	2.132	453.0	8.03	0.2435	–	Cal[17]
	38303	2.142	471.83	9.61	0.2412	0.53	Cal[39]
	38223.98	2.1330	454.24	–	0.2397	0.5443	Cal[19]
	38254.0	2.1239	449.96	–	0.259	–	Exp[40]

For ω_e and R_e of the $a^3\Pi$ state, these calculated results,[12,17,19,39] including ours, are basically consistent with experimental value.[40] However, for $X^1\Sigma^+$ and $a^3\Pi$ states, the calculated $\omega_e\chi_e$ by Brites *et al.*[39] is far from the experimental one.[40] Our result of $\omega_e\chi_e$ is closer to Yang *et al.*'s[39] value for $a^3\Pi$, but the error with respect to the experimental value is more than 20%. This is because in this paper three lowest states of AlCl are calculated, and those states have cross interaction with each other. In fact, if other higher electron states are considered, there will be more cross interactions.

As for the $A^1\Pi$ state, it can be seen that the difference of ω_e is large. Our simulation shows that this state has a deep potential well and a very small potential barrier. The potential well is located at 38436.3652 cm^{-1} above the ground state, and the potential barrier is located at 42901.400 cm^{-1} above the ground state at 2.95 Å. The ω_e is 453.43 cm^{-1} obtained by fitting the data of near equilibrium bond distance, which is consistent with the experimental result.[40]

3.2. The PECs and spectroscopic constants of Ω States

After considering the effect of SOC, three Λ–S states is divided into six Ω states, which include one 2 state, two 1 state, two 0^+ states, and one 0^- state. PECs of six Ω states are shown in Fig. 2. The initial dissociation channel $Al(^2P_u) + Cl(^2P_u)$ produces four new dissociation channels, *i.e.*, $Al(^2P_{3/2}) + Cl(^2P_{3/2})$, $Al(^2P_{1/2}) + Cl(^2P_{1/2})$, $Al(^2P_{1/2}) + Cl(^2P_{3/2})$, and $Al(^2P_{3/2}) + Cl(^2P_{1/2})$.

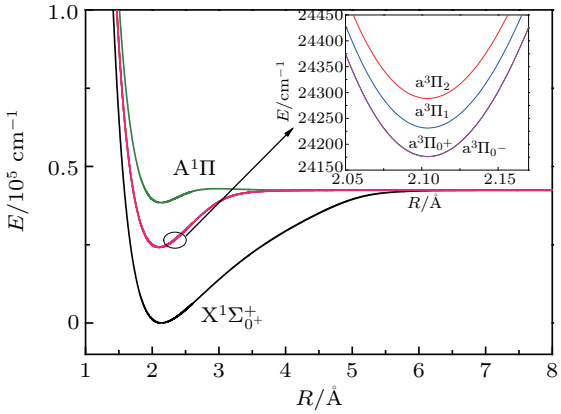

Fig. 2. Potential energy curves of Ω state.

The $X^1\Sigma^+_{0^+}$ and $A^1\Pi_1$ states are composed of $X^1\Sigma^+$ and $A^1\Pi$ in the Franck–Condon region. That is to say, when considering the SOC effect, $X^1\Sigma^+$ and $A^1\Pi$ states are not divided. The spectroscopic constants of Ω state are listed in Table 2. For the $X^1\Sigma^+_{0^+}$ state, the anharmonic vibrational frequency $\omega_e\chi_e$ is calculated to be 2.0110 cm^{-1}, and the corresponding difference is 0.0002 cm^{-1} with respect to the $X^1\Sigma^+$ state. The $X^1\Sigma^+_{0^+}$ and $X^1\Sigma^+$ states have the same values of equilibrium bond distance R_e, the harmonic frequency ω_e, and rotational constants B_e. The value of $\omega_e = 453.42$ cm^{-1} is also in good accordance with the datum of 455.6 cm^{-1} obtained by Wan *et al.*[19] Additionally, Wan *et al.*[19] calculated the values of R_e, B_e, and D_e for $X^1\Sigma^+_{0^+}$ and $A^1\Pi_1$ states by using the ACVQZ basis set, which are in good agreement with our result. Nonetheless, our basis set (AWCV5Z) can better reflect the core–valence correlation and describe the molecular orbitals. Therefore, our calculated values are more reliable.

The Λ–S state $^3\Pi$ is split into four states under the SOC effect ($^3\Pi_{0^-}$, $^3\Pi_{0^+}$, $^3\Pi_1$, and $^3\Pi_2$). The energy sequence of these four Ω states from high to low is 2, 1, 0^+, and 0^-. The energy interval of $a^3\Pi_{0^+} - a^3\Pi_1$ and $a^3\Pi_1 - a^3\Pi_2$ are 58.8453 cm^{-1} and 55.6518 cm^{-1}, respectively. And yet, as seen in Table 2, the excitation energy interval of $a^3\Pi_{0^-} - a^3\Pi_{0^+}$ is close to 0 cm^{-1}. For $a^3\Pi_{0^-}$, $a^3\Pi_{0^+}$, $a^3\Pi_1$, and $a^3\Pi_2$ electronic states, their potential well depths are calculated to be 2.2636 eV, 2.2705 eV, 2.2253 eV, and 2.2576 eV, respectively. Moreover, comparing with the $a^3\Pi$ state, the spectroscopic constants of four states do not change significantly, considering the SOC effect. For example, the spectroscopic constants of $a^3\Pi$ and $a^3\Pi_1$ states are almost the same.

Overall, the differences in spectroscopic constant between $X^1\Sigma^+$, $a^3\Pi$, $A^1\Pi$, and $X^1\Sigma^+_{0^+}$, $a^3\Pi_{0^-,0^+,1,2}$, $A^1\Pi_1$ are very small, which imples that the SOC effect has a weak influence on spectroscopic constant. So none of them is to be considered in the next calculations.

Table 2. Spectroscopic constants of Ω state.

States	T_e/cm^{-1}	R_e/Å	ω_e/cm^{-1}	$\omega_e\chi_e$/cm^{-1}	B_e/cm^{-1}	D_e/eV	References
$X^1\Sigma^+_{0^+}$	0	2.1366	481.83	2.0110	0.2425	5.2550	this work
	0	2.1374	478.13	–	0.2408	5.2072	Cal[18]
$a^3\Pi_{0^-}$	24168.3222	2.1034	527.51	2.6515	0.2502	2.2636	this work
	23905.13	2.1049	525.82	–	0.2484	2.2531	Cal[18]
$a^3\Pi_{0^+}$	24168.6075	2.1034	527.51	2.6515	0.2502	2.2705	this work
	23905.41	2.1049	525.82	–	0.2484	2.2898	Cal[18]
$a^3\Pi_0$	24793.100	–	–	–	0.2501	–	Cal[12]
$a^3\Pi_1$	24223.6298	2.1035	527.37	2.6538	0.2501	2.2253	this work
	24855.460	–	–	–	0.2518	–	Cal[12]
	23959.97	2.1050	525.68	–	0.2483	2.2448	Cal[18]
$a^3\Pi_2$	24279.2885	2.1036	527.24	2.6563	0.2501	2.2576	this work
	24919.752	–	–	–	0.2535	–	Cal[12]
	24015.17	2.1050	525.55	–	0.2483	2.2472	Cal[18]
$A^1\Pi_1$	38436.8261	2.1324	453.42	9.1289	0.2435	0.5013	this work
	38224.44	2.1330	455.6	–	0.24078	0.5443	Cal[18]

3.3. PDMs and TDMs

The PDMs for Λ–S states as a function of equilibrium bond distance at MRCI + Q level are depicted in Fig. 3. The PDM for $X^1\Sigma^+$, $a^3\Pi$, and $A^1\Pi$ states at R_e are 0.3543 a.u. (atomic unit), 0.6966 a.u., and 0.5263 a.u., respectively. For the ground state, the curve drops to a minimum value of −4.1222 a.u. at about 4.1 Å, then rises to 0. The PDM function of $a^3\Pi$ state reaches a minimum value of about −1.4223 a.u. at 2.7 Å, and then drops to zero at approximately 6.00 Å for this state. There are minimum and maximum value of PDM for $A^1\Pi$ state at 2.26 Å and 3.05 Å.

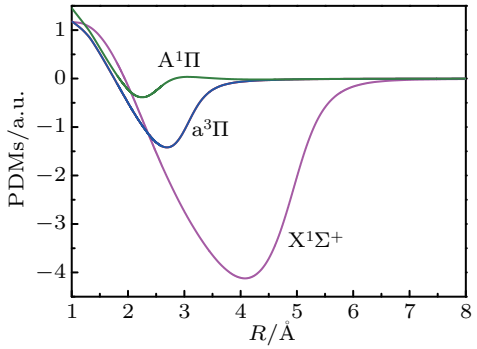

Fig. 3. PDM of $X^1\Sigma^+$, $a^3\Pi$, and $A^1\Pi$ states.

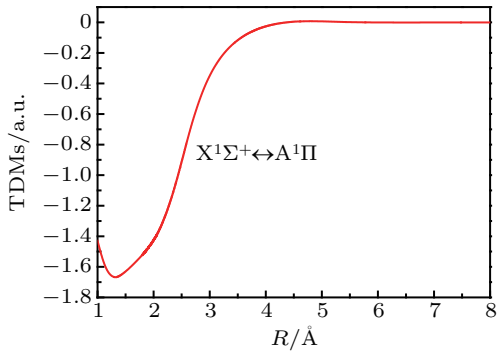

Fig. 4. TDM of $A^1\Pi \rightarrow X^1\Sigma^+$ transition.

The spin-allowed $A^1\Pi \rightarrow X^1\Sigma^+$ transition as a function of internuclear distance R is described in Fig. 4, and some TDM data are listed in Table 3. The TDM of $A^1\Pi \rightarrow X^1\Sigma^+$ transition first decreases to a minimum value of 1.6705 a.u. at 1.3 Å, then rises quickly and reaches 0 at about 4.35 Å. Then there is a small increase of 4.8 Å to a maximum value of 0.0074 a.u., and finally tends to 0. The TDM of the $A^1\Pi \rightarrow X^1\Sigma^+$ transition system has been calculated with ab initio method by Yang *et al.*[39] at an MRCI level in a range of 1 Å $\leq R \leq$ 11 Å and by Wan *et al.*[19] in a valid range of 1 Å $\leq R \leq$ 8 Å at an MRCI + Q level. These results are compared with our values of TDM in the range of 1 Å $\leq R \leq$ 8 Å at the MRCI + Q/AWCV5Z-DK /4220 level. Our results are close to those calculations. In addition, it is clear that the TDM function of the $A^1\Pi \rightarrow X^1\Sigma^+$ transition tends to zero at large internuclear distance, because of the orbit-forbidden transition at the atomic limit.

Table 3. TDM function of $A^1\Pi \rightarrow X^1\Sigma^+$transition.

R/Å	TDM/a.u.	R/Å	TDM/a.u.
1.00	–1.4292	2.20	–1.2721
1.10	–1.5694	2.24	–1.2327
1.20	–1.6487	2.28	–1.1905
1.30	–1.6705	2.32	–1.1454
1.40	–1.6574	2.36	–1.0974
1.50	–1.6302	2.40	–1.0468
1.60	–1.5970	2.44	–0.9939
1.65	–1.5791	2.48	–0.9392
1.70	–1.5605	2.52	–0.8836
1.75	–1.5413	2.56	–0.8277
1.80	–1.5212	2.60	–0.7724
1.82	–1.5128	2.65	–0.7053
1.84	–1.5043	2.70	–0.6414
1.86	–1.4956	2.80	–0.5261
1.88	–1.4866	2.90	–0.4288
1.90	–1.4774	3.00	–0.3485
1.92	–1.4678	3.20	–0.2282
1.94	–1.4579	3.40	–0.1467
1.96	–1.4476	3.60	–0.0907
1.98	–1.4368	3.80	–0.0522
2.00	–1.4255	4.00	–0.0261
2.04	–1.4011	4.20	–0.0092
2.08	–1.3738	4.40	–0.0010
2.12	–1.3431	…	…
2.16	–1.3091	…	…

Table 4. Values of vibrational level G_v and rotational constant B_v of $X^1\Sigma^+$, $a^3\Pi$, and $A^1\Pi$ states.

	$X^1\Sigma^+$				$a^3\Pi$		$A^1\Pi$				
	This work	Cal[16]	Cal[18]	This work	This work	This work	This work	Cal[16]	Cal[17]	This work	Cal[12]
v	G_v/cm^{-1}	G_v/cm^{-1}	G_v/cm^{-1}	B_v/cm^{-1}	G_v/cm^{-1}	B_v/cm^{-1}	G_v/cm^{-1}	G_v/cm^{-1}	G_v/cm^{-1}	B_v/cm^{-1}	B_v/cm^{-1}
0	240.5010	246.6	240.9387	0.24161783	263.1362	0.24932508	224.9823	232.1	223.9	0.24216279	0.24410415
1	718.7952	734.1	718.5298	0.23993335	786.1168	0.24770207	671.5638	685.3	662.7	0.23951306	0.24148210
2	1192.5451	1217.3	1191.9767	0.23831481	1302.6002	0.24607478	1105.2420	1126.7	1088.6	0.23672397	0.23869909
3	1662.0706	1698.0	1661.3180	0.23672528	1813.3884	0.24445907	1525.7333	1557.5	1505.2	0.23374497	0.23567850
4	2127.5010	2175.2	2126.5919	0.23515687	2318.8266	0.24285133	1932.1190	1975.3	1912.6	0.23052709	0.23240610
5	2588.9148	2648.4	2587.8364	0.23360431	2819.0778	0.24124801	2323.2072	2379.2	2308.6	0.22701603	0.22879390
6	3046.3716	3117.3	3045.0888	0.23206585	3314.2468	0.23964520	2697.5628	2768.5	2690.4	0.22314009	0.22482860
7	3499.9251	3581.7	3498.3862	0.23054037	3804.3924	0.23804375	3053.3913	3141.7	3055.0	0.21878900	–
8	3949.6157	4041.8	3947.7651	0.22902616	4289.5436	0.23644081	3388.3535	3496.6	3397.4	0.21379064	–
9	4395.4891	4497.6	4393.2617	0.22752282	4769.7205	0.23483504	3699.2661	3830.5	3711.1	0.20785838	–
10	4837.5825	–	4834.9118	0.22603005	5244.9300	0.23322586	–	–	–	–	–
11	5275.9336	–		0.22454753	5715.1661	0.23161206	–	–	–	–	–
12	5710.5784	–		0.22307481	6180.4184	0.22999195	–	–	–	–	–
13	6141.5546	–		0.22161239	6640.6696	0.22836470	–	–	–	–	–
14	6568.8977	–		0.22015955	7095.8901	0.22672946	–	–	–	–	–
15	6992.6416	–		0.21871493	7546.0501	0.22508469	–	–	–	–	–
16	7412.8091	–		0.21727858	7991.1156	0.22342776	–	–	–	–	–
17	7829.4287	–		0.21585131	8431.0264	0.22175553	–	–	–	–	–
18	8242.5418	–		0.21443543	8865.6963	0.22006161	–	–	–	–	–
19	8652.1922	–		0.21302762	9295.0268	0.21834814	–	–	–	–	–

The $X^1\Sigma^+$, $a^3\Pi$, and $A^1\Pi$ states have well depth of 42439.744 cm^{-1}, 18235.2380 cm^{-1}, and 4000.4776 cm^{-1}, which possess 159, 53, and 10 vibrational levels, respectively. The values of vibrational level G_v and rotational constant B_v of these three states are evaluated in this paper. For clarity, some yalues of G_v and B_v are listed in Table 4. The G_v values of the first 10 vibrational levels of $X^1\Sigma^+$ and $A^1\Pi$ states were reported by Langhoff *et al.*[16] through using the ANO basis set. Brites *et al.*[17] also calculated the G_v values for $A^1\Pi$ state ($v \leq 9$) with cc-pVQZ basis set. Until recently, the accurate G_v ($v \leq 10$) was computed by Yousefi and Bernath[18] by using a larger basis set (AWCV5Z) and active space (6330). It is clear from Table 4 that our results are fairly close to the calculated values of Yousefi and Bernath. It may imply that the predicted values of $a^3\Pi$ and $A^1\Pi$ states are reliable.

The electronic configuration is primarily characterized by $8\sigma^2 3\pi^4 9\sigma^2$ close to the equilibrium bond distance for the $X^1\Sigma^+$ state. And the dominant electronic configurations of states $a^3\Pi$ and $A^1\Pi$ are both $8\sigma^2 3\pi^4 9\sigma^1 4\pi^1$. Thus, the dominant electronic transition from $X^1\Sigma^+$ to $A^1\Pi$ state is $9\sigma^2$–$9\sigma^1 4\pi^1$. Additionally, we report that the R_e of the $A^1\Pi$ state is 2.1324 Å, while that of the $X^1\Sigma^+$ state is 2.1366 Å. Obviously, their values are very close to each other. Furthermore, the PECs of the two states are similar to each other, and both states have deep wells. According to these results, the FC principle predicts that the emissions of the $A^1\Pi \rightarrow X^1\Sigma^+$ system should be strong. To prove this, Einstein coefficients of emissions and FCFs are calculated at vibrational energy levels ($v' = 0$–$9 \rightarrow v'' = 0$–19) subsequently.

3.4. FCFs and radiative lifetimes

FCFs can be used to describe the overlap degree of vibrational wave functions for the transition. The FCFs $f_{v'v''}$ and Einstein coefficients $A_{v'v''}$ of the $A^1\Pi \rightarrow X^1\Sigma^+$ transition are calculated via the LEVEL8.2 program.[36] Tables 5 and 6 list the values of FCFs and $A_{v'v''}$ including $v'' = 0$–$19 \rightarrow v' = 0$–9 transition bands. These results confirm the expectations from the FC principle. It also shows that the $A^1\Pi$ state is not difficult to measure via spectroscopy. The $A^1\Pi \rightarrow X^1\Sigma^+$ transition has highly diagonal FCF ($f_{00} = 0.9988$). It can be seen from Table 6 that the larger $A_{v'v''}$ are located in the Frank–Condon region, and the maximum value (2.0101×10^8 s^{-1}) corresponds to the strong transition $v'' = 0 \rightarrow v' = 0$. The $A_{v'v''}$ values of $A^1\Pi \rightarrow X^1\Sigma^+$ system were determined by Langhoff *et al.*[16] over $v'' = v' = 0$–9 bands. Since Langhoff *et al.*[16] used a different basis set and did not consider the Davidson correction in calculations, leading their results to be a little different from ours.

Table 5. Values of FCF $f_{v'v''}$ of $A^1\Pi \rightarrow X^1\Sigma^+$ system. The presentation 4.83E-04 represents 4.83×10^{-4}.

	v'									
v''	0	1	2	3	4	5	6	7	8	9
0	9.98818E-01	4.78398E-04	7.02167E-04	3.93479E-07	7.65606E-07	4.04341E-09	9.98359E-10	1.25341E-10	2.68452E-10	2.90556E-11
1	4.83085E-04	9.97050E-01	3.33554E-05	2.40752E-03	2.11426E-05	4.24431E-06	2.41690E-07	4.46699E-09	9.48790E-10	4.30073E-10
2	6.97422E-04	1.32114E-05	9.90518E-01	3.71767E-03	4.84926E-03	1.94770E-04	7.52220E-06	2.46635E-06	1.14518E-08	1.27727E-08
3	4.97626E-08	2.44533E-03	2.61199E-03	9.66779E-01	2.05176E-02	6.71497E-03	9.19552E-04	6.63664E-07	1.04913E-05	8.55646E-07
4	1.17164E-06	5.14602E-06	6.01882E-03	1.34453E-02	9.08330E-01	6.35673E-02	5.73236E-03	2.81999E-03	5.42319E-05	1.68746E-05
5	3.74144E-10	7.45396E-06	8.08981E-05	1.29957E-02	3.74052E-02	7.95211E-01	1.46484E-01	1.33274E-03	5.78023E-03	6.71632E-04
6	9.70125E-10	3.07578E-08	3.41008E-05	5.07027E-04	2.61463E-02	7.55857E-02	6.14160E-01	2.70873E-01	2.69087E-03	6.71398E-03
7	2.89228E-10	1.95468E-08	8.15068E-07	1.38301E-04	2.14335E-03	4.93954E-02	1.19302E-01	3.77128E-01	4.02400E-01	3.94308E-02
8	2.13923E-12	1.98870E-09	1.83340E-07	8.03659E-06	5.22032E-04	7.13862E-03	8.59514E-02	1.45070E-01	1.42814E-01	4.51398E-01
9	6.69574E-12	8.48300E-13	1.55759E-08	1.36773E-06	5.34629E-05	1.83860E-03	1.98267E-02	1.32097E-01	1.22057E-01	9.38377E-03
10	5.17926E-12	8.20495E-13	3.35608E-10	1.37589E-07	9.05185E-06	2.84213E-04	5.95663E-03	4.63574E-02	1.66130E-01	4.88444E-02
11	1.41060E-15	2.60931E-11	6.43941E-11	9.92440E-09	1.16642E-06	5.42910E-05	1.28672E-03	1.73157E-02	8.85275E-02	1.45997E-01
12	6.41949E-13	1.17781E-12	8.41692E-11	1.55275E-09	1.36483E-07	8.95216E-06	2.95292E-04	5.05287E-03	4.33348E-02	1.26296E-01
13	1.51360E-13	1.10972E-12	3.93025E-12	3.86432E-10	2.12482E-08	1.41243E-06	6.16763E-05	1.44210E-03	1.69884E-02	8.65143E-02
14	1.58393E-14	1.26886E-12	7.10337E-13	1.92797E-14	3.49037E-09	2.43779E-07	1.24081E-05	3.80785E-04	6.18321E-03	4.65076E-02
15	5.16593E-14	6.32918E-14	4.45319E-12	6.73608E-13	1.74731E-10	4.17134E-08	2.53420E-06	9.62639E-05	2.07753E-03	2.22145E-02
16	3.02845E-15	5.41022E-14	7.08558E-13	7.27166E-12	5.46917E-11	5.20747E-09	5.07411E-07	2.39518E-05	6.61912E-04	9.65683E-03
17	1.07037E-14	4.25300E-14	1.35711E-13	9.87509E-13	2.36995E-11	1.07211E-09	9.26877E-08	5.82832E-06	2.04113E-04	3.92877E-03
18	1.32887E-14	2.93735E-15	5.49662E-13	6.12618E-14	7.98490E-13	2.31615E-10	1.95042E-08	1.36617E-06	6.12376E-05	1.52672E-03
19	3.05316E-16	6.50543E-16	1.70132E-13	6.68551E-13	2.57150E-13	9.26024E-12	4.01243E-09	3.30297E-07	1.78928E-05	5.72960E-04

Table 6. Values of Einstein coefficient $A_{v'v''}$ of $A^1\Pi(v'=0\text{–}9)$–$X^1\Sigma^+(v''=0\text{–}19)$ transition bands (in unit s^{-1}). The presentation 2.01E+08 represents 2.01×10^8.

	v'									
v''	0	1	2	3	4	5	6	7	8	9
0	2.0101E+08	1.7285E+04	1.5662E+05	1.3331E+03	1.0708E+02	6.7239E+00	2.3117E-01	2.2432E-01	4.4606E-02	5.9189E-03
1	5.6353E+05	1.9545E+08	5.0472E+05	4.7179E+05	1.4743E+04	3.9324E+02	9.9913E+01	1.4873E+00	1.7356E-01	2.6602E-01
2	1.2779E+05	3.7009E+05	1.8888E+08	2.6086E+06	8.1453E+05	7.9165E+04	1.5267E+02	6.0722E+02	3.3175E+01	1.2921E-01
3	3.8249E+02	4.0139E+05	2.3205E+04	1.7914E+08	8.0286E+06	9.0127E+05	2.7373E+05	1.9964E+03	1.6348E+03	3.7087E+02
4	1.5476E+02	1.3164E+02	8.7843E+05	2.8087E+05	1.6352E+08	1.8804E+07	4.7460E+05	6.5959E+05	3.8910E+04	8.6982E+02
5	2.3981E+00	8.4234E+02	1.3101E+03	1.6901E+06	1.8673E+06	1.3938E+08	3.6330E+07	2.7159E+03	1.0570E+06	2.2898E+05
6	5.1887E-01	1.2777E+00	3.2835E+03	2.1448E+04	3.0603E+06	5.0697E+06	1.0556E+08	5.9081E+07	2.0589E+06	8.3176E+05
7	1.4092E-02	3.7852E+00	1.0991E+01	1.1563E+04	1.2146E+05	5.2781E+06	9.0998E+06	6.4909E+07	7.9316E+07	1.2117E+07
8	1.8600E-02	3.2735E-02	1.9263E+01	2.8237E+02	3.9095E+04	4.5612E+05	8.5059E+06	1.1650E+07	2.6485E+07	8.2164E+07
9	1.2164E-03	3.8976E-02	2.8702E-01	9.7396E+01	2.4171E+03	1.2710E+05	1.3294E+06	1.2251E+07	9.8120E+06	3.4030E+06
10	1.3290E-03	1.2427E-02	1.3411E-02	3.7690E+00	5.1655E+02	1.4058E+04	3.8837E+05	3.1431E+06	1.4564E+07	3.6775E+06
11	1.1465E-03	1.7135E-03	5.3322E-02	1.3197E-01	3.98920E+01	2.7526E+03	6.5476E+04	1.0778E+06	5.9357E+06	1.2193E+07
12	3.6751E-05	3.9972E-03	1.5503E-03	2.2087E-01	3.8621E+00	3.3554E+02	1.4025E+04	2.5686E+05	2.5873E+06	8.2485E+06
13	1.1859E-04	6.6434E-04	7.1485E-03	3.2595E-03	1.2429E+00	4.6169E+01	2.3748E+03	6.5613E+04	8.4842E+05	4.9529E+06
14	1.0091E-04	1.1781E-04	2.2982E-03	6.4078E-03	5.0473E-02	9.3943E+00	4.1703E+02	1.4617E+04	2.7133E+05	2.2554E+06
15	3.1850E-06	4.1651E-04	8.2120E-05	6.0060E-03	5.0384E-04	8.8676E-01	8.2457E+01	3.2167E+03	7.8252E+04	9.3930E+05
16	1.2557E-05	1.2358E-04	8.4387E-04	1.0931E-05	1.6821E-02	6.7554E-02	1.2336E+01	7.2473E+02	2.1695E+04	3.5322E+05
17	1.0092E-05	1.3355E-06	3.1943E-04	8.2781E-04	7.7536E-05	6.7331E-02	1.8707E+00	1.4666E+02	5.9239E+03	1.2516E+05
18	4.6008E-08	5.0389E-05	1.7575E-06	6.7005E-04	8.0986E-04	4.8178E-04	5.6654E-01	2.9770E+01	1.5317E+03	4.2759E+04
19	2.3732E-06	3.7032E-05	1.2095E-04	3.3838E-05	1.3507E-03	9.2345E-05	4.5467E-02	7.2513E+00	3.9104E+02	1.3999E+04

The radiative lifetimes for all vibrational levels of the $A^1\Pi$ state are estimated by using $A_{v'v''}$ and are summarized in Table 7. Rogowski and Fontijn[41] determined the lifetime of $A^1\Pi$ $v'=0$ band to be about 6.4 ± 2.5 ns in experiment. According to Table 7, the radiative lifetimes of all vibrational levels are about 10^{-9} s. The magnitude of lifetime of $v'=0$ band is the same as the experimental value,[41] both of which are 10^{-9} s. Langhoff *et al.*[16] calculated the lifetimes of the $v'=0$–9 at the MRCI/ANO level. The maximum difference between our result and their result is 5.2856% for $v'=9$ energy level. In addition, some theoretical values were obtained only for lower vibrational levels by Yang *et al.*[39] at the MRCI+Q/ACVQZ level. Our values are of the same order of magnitude as theirs, but we believe that our results are more accurate because the larger basis set (AWCV5Z) is used. Based on $A_{v'v''}$ of the $A^1\Pi\rightarrow X^1\Sigma^+$ transition and radiative lifetime, the $A^1\Pi$ state should be easily detectable in the spectrum.

Table 7. Values of radiative lifetime τ'_v (in unit ns) for vibrational levels ($v'=0$–9) of $A^1\Pi$ state.

v'	This work	Cal[16]	Cal[39]	Exp[41]
0	4.9578	5.17	5.04	6.4±2.5
1	5.0958	5.28	5.19	–
2	5.2507	5.40	5.35	–
3	5.4283	5.55	5.54	–
4	5.6348	5.73	5.76	–
5	5.8783	5.92	–	–
6	6.1710	6.15	–	–
7	6.5309	6.42	–	–
8	6.9889	6.76	–	–
9	7.6018	7.20	–	–

The relationship between line intensities and wavenumber of the $A^1\Pi\rightarrow X^1\Sigma^+$ transition is determined based on FCFs, and the results are shown in Fig. 5. For atmospheric applications, the computational values are divided into R and P branches up to $J''=16$ at 296 K for the $A^1\Pi\rightarrow X^1\Sigma^+$ transition. Figure 5 shows that the absolute line intensities change with the decrease of wavenumber, and the curve shows a trend of first increase and then decrease. The difference between the highest point and other points is large, which causes the highest point to be prominent. That is, when $\Delta v=+1$, the $A^1\Pi\rightarrow X^1\Sigma^+$ transition f_{10}, f_{21}, f_{32}, and f_{43} are dramatically higher than other FCFs. These results show that $v'=2-v''=1$ band is the strongest excitation. For 2–1 band of $A^1\Pi\rightarrow X^1\Sigma^+$ system, the maximum value of line intensities is 5.4807×10^{-37} $cm^{-1}/(molecule\cdot cm^{-2})$ corresponding to the position 38822.2939 cm^{-1} (P(1)). So far, these line intensities have not been reported yet. But we hope that our results will be useful for analyzing interstellar AlCl based on emission from $A^1\Pi\rightarrow X^1\Sigma^+$.

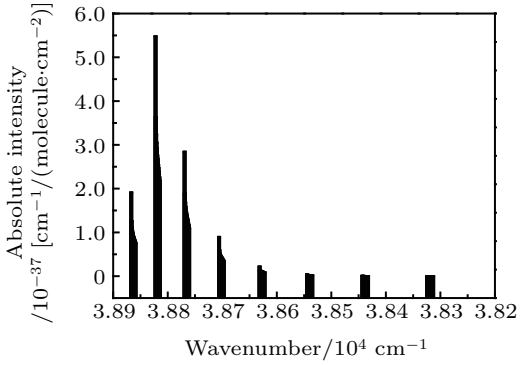

Fig. 5. Absolute line intensities of $\Delta v=+1$ transition bands of $A^1\Pi\rightarrow X^1\Sigma^+$ system.

4. Conclusions

Based on the MRCI + Q method with aug-cc-pwCV5Z-DK basis set and 4220 active space, the PECs, spectroscopic constants, PDMs, TDM, and vibrational levels for the three Λ–S states of AlCl are studied. In addition, the PECs and spectroscopic constants of six Ω states, *i.e.*, $X^1\Sigma^+_{0^+}$, $a^3\Pi_{0^-}$, $a^3\Pi_{0^+}$, $a^3\Pi_1$, $a^3\Pi_2$, and $A^1\Pi_1$, are determined. The results show that the SOC effect has little influence on spectroscopic constants of these states. According to TDMs combined with PECs, Einstein coefficients $A_{v'v''}$, FCFs, and radiative lifetime τ'_v are determined, and these results are close to the existing theoretical and experimental data.

The radiative lifetime of $A^1\Pi$ state is about 10^{-9} s, which is very short. That is, the spontaneous emissions should be very strong, and the emissions of the $A^1\Pi \rightarrow X^1\Sigma^+$ system should not be difficult to detect. Moreover, the line intensity of the $A^1\Pi \rightarrow X^1\Sigma^+$ system $\Delta v = +1$ transition band is predicted, and the results show that 2–1 band is the strongest excitation. We expect that our theoretical calculations will be helpful in the further study of interstellar AlCl and even other system transitions. It is also useful to analyze other theoretical spectrum properties, especially ro-vibrational transitions or high overtone bands.

References

[1] Tsuji T 1973 *A&A* **23** 411
[2] Cernicharo J and Guélin M 1987 *A&A* **183** L10
[3] Ziurys L M 2006 *Proceeding of the National Academy of Sciences* **103** 12274
[4] Agúndez M, Fonfría J P, Cernicharo J, Kahane C, Daniel F and Guélin M 2012 *A&A* **543** A48
[5] Decin L, Richards A M S, Waters L B F M, Danilovich T, Gobrecht D, Khouri T, Homan W, Bakker J M, Van de Sande M, Nuth J A and De Beck E 2017 *A&A* **608** A55
[6] Asplund M, Grevesse N, Sauval A J and Scott P 2009 *Ann. Rev. Astron. Astrophys.* **47** 481
[7] Bhaduri B N and Fowler A 1934 *Proceedings of the Royal Society of London* **145** 321
[8] Mahanti P C 1934 *Z. Phys.* **88** 550
[9] Wyse F C and Gordy W 1972 *J. Chem. Phys.* **56** 2130
[10] Hedderich H G, Dulick M and Bernath P F 1993 *J. Chem. Phys.* **99** 8363
[11] Hildenbrand D L and Theard L P 1969 *J. Chem. Phys.* **50** 5350
[12] Ram R S, Rai S B, Upadhya K N and Rai D K 1982 *Phys. Scr.* **26** 383
[13] Mahieu E, Dubois I and Bredohl H 1989 *J. Mol. Spectrosc.* **134** 317
[14] Mahieu E, Dubois I and Bredohl H 1989 *J. Mol. Spectrosc.* **138** 264
[15] Saksena M D, Dixit V S and Singh M 1998 *J. Mol. Spectrosc.* **87** 1
[16] Langhoff S R, Bauschlicher Jr C W and Taylor P R 1988 *J. Chem. Phys.* **88** 5715
[17] Brites V, Hammoutène D and Hochlaf M 2008 *J. Phys. Chem. A.* **112** 13419
[18] Yousefi M and Bernath P F 2018 *Astrophys. J. Suppl. Ser.* **237** 8
[19] Wan M, Yuan D, Jin C, Wang F, Yang Y, Yu Y and Shao J 2016 *J. Chem. Phys.* **145** 024309
[20] Werner H J, Knowles P J, Knizia G, Manby F R and Schütz M 2018 *MOLPRO, a package of ab initio programs*, see http://www.molpro.net
[21] Werner H J and Knowles P J 1985 *J. Chem. Phys.* **82** 5053
[22] Knowles P J and Werner H J 1985 *Chem. Phys. Lett.* **115** 259
[23] Langhoff S R and Davidson E R 1974 *Int. J. Quantum Chem.* **8** 61
[24] Knowles P J and Werner H J 1988 *Chem. Phys. Lett.* **145** 514
[25] Werner H J and Knowles P J 1988 *J. Chem. Phys.* **89** 5803
[26] Douglas M and Kroll N M 1974 *Ann. Phys.* **82** 89
[27] Hess B A 1986 *Phys. Rev. A* **33** 3742
[28] Berning A, Schweizer M, Werner H J, Knowles P J and Palmieri P 2000 *Mol. Phys.* **98** 1823
[29] Yin Y, Shi D, Sun J and Zhu Z 2018 *Astrophys. J. Suppl. Ser.* **236** 34
[30] Cheng J, Zhang H and Cheng X 2018 *Astrophys. J.* **859** 19
[31] Yin Y, Shi D, Sun J and Zhu Z 2018 *Astrophys. J. Suppl. Ser.* **235** 25
[32] Xing W, Shi D, Sun J and Zhu Z 2018 *Astrophys. J. Suppl. Ser.* **237** 16
[33] Woon D E and Dunning T H Jr 1993 *J. Chem. Phys.* **98** 1358
[34] De Jong W A, Harrison R J and Dixon D A 2001 *J. Chem. Phys.* **114** 48
[35] Peterson K A and Dunning Jr T H 2002 *J. Chem. Phys.* **117** 10548
[36] Le Roy R J 2015 *LEVEL 8.2: A computer program for solving the radial Schrodinger equation for bound and quasibound levels*, Chemical Physics Research Report No. CP-668, (University of Waterloo)
[37] Bernath P F 2005 *Spectra of Atoms and Molecules*, 2nd ed. Oxford : Oxford University Press
[38] Castano F, de Juan J and Martinez E 1983 *J. Chem. Educ.* **60** 91
[39] Yang R, Tang B and Gao T 2016 *Chin. Phys. B* **25** 043101
[40] Herzberg G and Huber K P 1979 *Constants of Diatomic Molecules, Molecular Spectra and Molecular Structure*, Vol. IV
[41] Rogowski D F and Fontijn A 1987 *Chem. Phys. Lett.* **137** 219